

Optimization of Concentrated Solar Power Systems with Thermal Storage for Enhanced Efficiency and Cost-Effectiveness in Thermal Power Plants

Abdulaziz Alanazi

Department of Electrical Engineering, College of Engineering, Northern Border University, Arar, Saudi Arabia

af.alanazi@nbu.edu.sa

Received: 9 September 2023 | Revised: 1 October 2023 | Accepted: 10 October 2023

Licensed under a CC-BY 4.0 license | Copyright (c) by the authors | DOI: <https://doi.org/10.48084/etasr.6381>

ABSTRACT

The study presents a comprehensive investigation of solar thermal systems with varying capacities and Thermal Energy Storage (TES) durations in the existing fossil fuel-run Thermal Power Plant at Ar'Ar, Saudi Arabia. The main objective is to assess the feasibility, economic viability, and environmental impact of these systems for sustainable power generation. In pursuit of sustainable energy solutions, parabolic trough systems with capacities ranging from 10 MW to 50 MW and TES durations from 0 to 8 hours were analyzed. The evaluation includes thermal and electrical assessments, field performance evaluations, and detailed cost analysis for each configuration. Multi-Criteria Decision Making (MCDM) was utilized to identify the best TES for every Concentrated Solar Power (CSP) system with the 4 hr TES ranking first among all capacities. The research uncovers significant positive correlations between system capacity and thermal and electrical output. The 50 MW system exhibits the highest thermal output of 280.899 MW and electrical output of 180580 MW. Incorporating 4 hr TES emerges as a critical factor in enhancing system performance, optimizing the cost of electricity, and achieving a payback period within 12 years. Furthermore, the integration of solar thermal energy demonstrates substantial reductions in fossil fuel consumption. Across all capacities, the 4-hour TES system yields considerable fuel savings, ranging from 18.84 tons/hour for the 10 MW system to 96 tons/hour for the 50 MW system. These reductions correspondingly translate to considerable cost savings, with the 50 MW system reducing fuel costs by \$5760. Moreover, the study highlights the crucial environmental benefits of solar thermal systems, leading to substantial CO₂ emission reduction, with the 50 MW system achieving a reduction of 93452.8 kg/hour.

Keywords-concentrated solar power; capacity optimization; sustainable energy integration; techno-economic analysis; multi-criteria decision making; fossil fuel reduction

I. INTRODUCTION

The world's dependence on electricity as the backbone for growth and development is undeniable. In recent years, global energy consumption has skyrocketed to a staggering 25,300 TWh, with over 60% of electricity production derived from fossil fuels [1]. Coal is the leading source of fossil fuel-based electricity, accounting for 36% of the total, followed by natural gas at 22%. China has the highest number of operational coal power plants (1,118), followed by India (285) and the United States (225) [2]. Meanwhile, in the Middle East, power generation primarily relies on natural gas (68%) and oil (30%) operated power plants [3]. The significant carbon emissions from fossil fuel-based power generation are a major contributor to global warming and climate change and pose a serious threat to the environment. On average, coal and oil-run power plants emit 2-2.5 pounds/kWh of CO₂, while natural gas produces around 0.9 pounds/kWh [4]. Moreover, these emissions are

accompanied by pollutants such as ashes, arsenic, lead, mercury, selenium, chromium, and cadmium, which can be harmful to the environment and public health [5].

Saudi Arabia, a prominent nation in the Middle East, occupies a strategic location and is home to a sizable population, making it one of the world's most significant energy consumers. With its rapid economic growth and urbanization, the country's energy demand has been steadily increasing over the years. Consequently, Saudi Arabia's energy sector faces the challenge of meeting the escalating energy requirements to fuel its industries, support its populace, and drive infrastructural development. The backbone of Saudi Arabia's energy sector has long been its vast reserves of fossil fuels, notably oil and natural gas [6]. These hydrocarbon resources have played a pivotal role in the country's economic prosperity and have positioned it as a global energy powerhouse. Saudi Arabia has large oil reserves and is the

highest exporter of oil, holding a crucial position in international energy markets [3]. Despite its economic benefits, the continued reliance on fossil fuel-based power generation poses significant challenges for Saudi Arabia. One of the most pressing concerns is the environmental impact, primarily associated with greenhouse gas emissions. The combustion of hydro carbon-based fuels releases greenhouse gases, especially CO₂ which are leading factors to climate change and global warming [8]. In line with international efforts to combat climate change, Saudi Arabia is under increasing pressure to reduce its carbon footprint and make the transition to cleaner alternative energy sources. Moreover, the volatility of global oil prices can place a strain on the country's budget and economy, impacting its fiscal stability and long-term planning. Additionally, the finite nature of fossil fuel reserves raises questions about the sustainability of the energy sector in the long run. While Saudi Arabia boasts significant reserves, prudent management of these resources and the exploration of alternative energy sources are essential to ensure energy security and stability in the future.

As a step toward a more sustainable energy future, Saudi Arabia has recognized the potential of renewable energy, particularly solar power [9]. Authors in [10] carried out an extensive investigation into the current state, growth, potential, and sustainability performance of different renewable technologies in Saudi Arabia, aligning their findings with the objectives of Saudi Vision 2030. They projected a substantial surge in electricity demand, reaching 120 GW by 2032, with an expected increase in oil production from 3.4 to 8.3 million barrels per day. Various renewable technologies, including wind, solar, geothermal, hydro, and biomass, were reviewed, with a particular focus on solar power, which has the potential to contribute 9500 MW to the energy landscape [11]. The research revealed Saudi Arabia's remarkable potential in solar and wind technologies, sufficient to meet energy needs for the next five decades. Additionally, the study highlighted the potential of offshore wind, biomass, and thermal energy in the country. Examining the economic aspects, authors in [12] conducted a comprehensive cost and savings assessment of renewable systems in Saudi Arabia. Their findings revealed that solar technology, owing to its rapid development, currently stands out as the most cost-effective and savings-driven option, followed closely by wind energy. The establishment of hydroelectric power stations continues to be costly and time-intensive due to the absence of inherent infrastructure. While technologies such as geothermal and fuel cells show potential, they currently involve substantial expenses and are not yet regarded as feasible substitutes. With an average of approximately 3,000 hours of sunshine per year, the country possesses abundant solar energy resources [13]. This high solar insolation creates an ideal environment for the deployment of solar energy technologies. Solar energy has two major technologies: Photovoltaic (PV) and Concentrated Solar Power (CSP) [14]. In PVs, the semiconductor material directly converts photons of light into electric energy [15], while CSP employs mirrors or lenses to concentrate sunlight onto a receiver, producing heat that drives a turbine to generate electricity [16]. Each technology has its advantages and suitability for different applications [17]. Given Saudi Arabia's

warm climate and high temperatures, CSP stands out as a promising renewable energy option [18]. Although PV technology's performance declines in high temperatures [19], CSP thrives on heat generating more output as temperature rises [20]. However, challenges remain in effectively integrating CSP into the existing energy infrastructure. One significant advantage of implementing CSP in Saudi Arabia lies in the country's already established infrastructure of Thermal Power Plants. By integrating CSP technology, these existing thermal plants can be modified and repurposed, eliminating the need for their closure. The principle of operation for both thermal power plants and CSP is centered around utilizing heat to produce steam that drives turbines for power generation [21, 22]. While thermal power plants rely on burning fossil fuels as the source of heat, CSP harnesses the sun's energy through mirrors and absorbers to generate the required heat [23]. This fundamental similarity between the two technologies enables their harmonious coexistence in a hybrid power plant setup.

In a hybrid power plant, the collectors of CSP serve as substitutes for the conventional burners in thermal power plants. As CSP captures and concentrates the sun's heat, it generates steam that drives the turbine, like the conventional setup [24]. Crucially, this integration requires minimal modifications to the pre-existing thermal power plants, ensuring significant cost savings compared to constructing entirely new, independent solar power plants. The essential components of the power plant, including the steam generator, turbine, power generator, condenser, and cooling tower, remain unchanged, leveraging the already present infrastructure and further reducing capital expenditures. Multiple studies have presented detailed modeling, analyses and approaches how this hybrid model can be physically implemented [25–27]. Moreover, the synergy between CSP and thermal power plants offers an added environmental benefit. During the periods the CSP is producing heat, the burning of hydro carbons fuels can be significantly reduced or even eliminated. This reduction in fossil fuel consumption translates to lower running costs and a substantial decrease in greenhouse gas emissions, aligning with the commitments to combat climate change and promote sustainable energy solutions.

The main focus and research problem addressed in this study are to analyze the feasibility of a hybrid power plant that combines fossil fuel and solar thermal energy in Saudi Arabia. The purpose is to investigate the potential advantages, challenges, and economic viability of such a hybrid system. The System Advisory Model (SAM) tool was employed for comprehensive analysis. Different capacities of CSP (ranging from 10 MW to 50 MW) will be studied to understand their impact on key performance metrics, such as green thermal output, electrical output, capacity factor, fossil fuel consumption reduction, cost savings, CO₂ emission reduction, Levelized Cost of Electricity (LCOE), Net Present Value (NPV), and revenue, in Saudi Arabia. However, the actual implementation and deployment of the hybrid power plant are beyond the scope of this research. The study will encompass all three major fossil fuel types: gas, coal, and oil, to account for the diverse energy mix in Saudi Arabia. Additionally, the research will evaluate the impact of introducing different heat

storage capacities (ranging from 0 to 8 hours) for each CSP capacity. An MCDM method was utilized to select the most suitable storage system for each capacity, considering the specific requirements and constraints. The findings of this study can provide valuable insights into the advantages and feasibility of a hybrid power plant that integrates fossil fuel-based thermal power plants with CSP in Saudi Arabia. By reducing fossil fuel consumption and greenhouse gas emissions, such a hybrid system can contribute to the country's sustainable energy goals while maintaining energy security and economic stability. This research introduces a novel approach in enhancing the sustainability of Saudi Arabia's energy sector by leveraging its existing fossil fuel-based infrastructure and integrating it with CSP. The study's focus on diverse CSP capacities, heat storage options, and MCDM methods adds novelty to the exploration of hybrid power plants in the context of a rapidly evolving energy landscape. The specific objectives of this research are:

- To evaluate the performance and efficiency of a hybrid power plant integrating CSP with fossil fuel-based thermal power plants.
- To assess the impact of different CSP capacities on key performance metrics, including green thermal output, electrical output, capacity factor, fossil fuel consumption reduction, cost savings, CO₂ emissions reduction, LCOE, NPV, and revenue.
- To consider all three major fossil fuel types (gas, coal, and oil) in the analysis to account for the diversity of the energy mix in Saudi Arabia.
- To explore the effect of introducing various heat storage capacities (ranging from 0 to 8 hours) for each CSP capacity, and identify the most suitable storage system using MCDM methods.

II. METHODOLOGY

A. Research Design

This study adopts a quantitative research design to thoroughly analyze the feasibility of a hybrid power plant that integrates CSP with existing fossil fuel-based thermal power plants. This quantitative approach ensures objective data collection and rigorous analysis of key performance metrics, facilitating a comprehensive assessment of the proposed hybrid system.

B. System Advisory Model (SAM) Simulation

To conduct the analysis, the study employs the SAM tool, a widely recognized simulation software utilized for evaluating renewable energy systems and assessing their economic viability [3]. SAM enables precise modeling of solar power plants, taking into account factors such as geographical location, local weather patterns, and solar resource availability. By using SAM, the hybrid power plant will be meticulously modeled, and its performance will be simulated under various scenarios to accurately determine key metrics, including electrical output, thermal output, capacity factor, and LCOE.

C. Empirical Model Option in SAM

In utilizing SAM, the study leverages the empirical model option, which incorporates a set of curve-fit equations derived from detailed analysis of data collected from real-life thermal power plants. This option offers realistic results while focusing primarily on the initial part of heat collection in the hybrid power plant. Given that an existing thermal power plant is under consideration, only the first two blocks, namely the Solar Field and the Thermal Storage, are designed. The empirical model ensures practical outcomes and provides insights into the integration of CSP within the existing infrastructure.

D. Geospatial Analysis and Site Selection

Geospatial analysis will be employed to identify potential locations for the hybrid power plant in Saudi Arabia. Factors such as solar resource availability, land availability, proximity to existing thermal power plants, and grid connection feasibility will be considered during the site selection process. The chosen site should optimize solar energy capture, streamline integration with the existing power infrastructure, and ensure minimal environmental impact.

E. Parabolic Trough Technology

In this study, the parabolic trough technology is employed to capture thermal energy from the sun [28]. The parabolic CSP consists of 3 major design blocks: Solar Field, Thermal Storage, and Power Block [18]. Since an established fossil fuel plant is being considered, the design of the Power Block is not necessary, as it already exists within the system. Consequently, default values are used for this component. Thus, the study's focus lies on designing the first two blocks, namely the Solar Field and Thermal Storage, and optimizing their integration with CSP.

F. Evaluation of Multiple CSP Capacities

To achieve a comprehensive evaluation of the hybrid system's performance, the study considers multiple CSP capacities, ranging from 10 MW to 50 MW. Each capacity is individually assessed to determine its suitability and economic viability for implementation in Saudi Arabia. This thorough assessment of various capacities aims to optimize the hybrid system's design and identify the most efficient configuration.

G. Incorporating Heat Storage

Recognizing the challenge of solar energy availability at night, the study introduces different heat storage capacities for each CSP capacity, spanning from 0 to 8 hours. The evaluation of heat storage options aims to assess their impact on the hybrid power plant's ability to provide continuous power generation, enhancing its overall efficiency and energy dispatch capabilities.

H. Techno-Economic Analysis

A detailed techno-economic analysis will be performed to evaluate the capital costs, operating costs, and maintenance costs associated with the hybrid power plant. Additionally, the LCOE will be calculated for each capacity of CSP integration, considering various financial parameters such as discount rates, inflation, and project lifetime. This analysis will offer a comprehensive understanding of the economic viability of the

hybrid system and its competitiveness compared to conventional power generation.

I. Multi-Criteria Decision-Making (MCDM)

To select a heat storage system for each CSP capacity, a systematic MCDM approach will be used. MCDM facilitates a comprehensive evaluation of multiple criteria, enabling the selection of optimal storage solutions based on various performance indicators [29]. The use of MCDM ensures a thorough and objective assessment of the heat storage options, aligning the hybrid system with the specific requirements and constraints of the project [30].

J. Evaluation of Fossil Fuel Types

To capture the diversity of Saudi Arabia's energy mix, the analysis encompasses all three major fossil fuel types: gas, coal, and oil [6]. Specific properties and associated costs of each fossil fuel type are taken into consideration during the evaluation of the hybrid system. This evaluation ensures a comprehensive understanding of the economic and environmental implications of integrating CSP with diverse fossil fuel sources [24].

K. Environmental Impact Assessment

An environmental impact assessment will be performed to quantify the potential environmental benefits of the hybrid power plant. This assessment will include the estimation of greenhouse gas emission reductions. The findings will contribute to a comprehensive sustainability evaluation and facilitate decision-making that aligns with environmental conservation goals [11]. The following equations are related to CSP for optimum design and calculating the result [16].

Heat gain:

$$Qu = Fr.Aa \left[\frac{(S-Ar)}{Aa.Ul(Ti-Ta)} \right] \quad (1)$$

The temperature of a collector's output is given by:

$$To = Ti + \frac{Qu}{m.Cp} \quad (2)$$

The number of loops required is given by:

$$\text{No. of loops} = \frac{\left[\frac{P_{th}}{\text{Output power collector}} \right]}{\text{No. of collectors per loop}} \quad (3)$$

Solar Multiple (SM):

$$SM = \frac{\text{Power cycle capacity}}{\text{Field capacity}} \quad (4)$$

Solar Field Heat Output:

$$Q_{sf, des} = \frac{W_{pb, des}}{\eta_{des}} \times SM \quad (5)$$

Thermal losses:

$$Q_{hl} = Q_{hl, ref} \frac{I_{bn}}{I_{bn, des}} F_{hl}, I_{bn} F_{hl}, T_{amb} F_{hl}, V_{wind} \quad (6)$$

Thermal losses to irradiation:

$$F_{hl}, I_{bn} = C_0 + C_1 \left(\frac{I_{bn}}{I_{bn, des}} \right) + C_2 \left(\frac{I_{bn}}{I_{bn, des}} \right)^2 + C_3 \left(\frac{I_{bn}}{I_{bn, des}} \right)^3 \quad (7)$$

Power output:

$$\text{Output}_{Net} = \text{Output}_{Gross} \times CF \quad (8)$$

Integrated solar thermal electricity-producing efficiency:

$$\eta_{se} = \frac{\Delta We - \sum_{i=1}^n W_{sub, i}}{Q_{solar} + \sum_{i=1}^n Q_{add, i}} \quad (9)$$

where ΔWe is the improved power output after solar replacement, Q_{solar} is the thermal energy input into the feedwater heater, $\sum_{i=1}^n W_{sub, i}$ is the improved power consumption by some equipment after replacement, $\sum_{i=1}^n Q_{add, i}$ is the improved thermal energy load in the boiler after replacement, Fr stands for collector heat removal factor, Aa stands for concentrator aperture area, Ar stands for receiver area, S stands for absorbed solar radiation, Ul stands for heat loss coefficient, Ta stands for the ambient temperature, To is the outlet temperature (391°C), Ti is the inlet temperature (293°C in our case), m is the mass flow rate of the Heat Transfer Fluid-HTF (12 kg/s nominal), Cp is the specific heat capacity of the HTF, $Q_{sf, des}$ is the heat output from a solar field, $W_{pb, des}$ is the design work from a power block, η_{des} is the designed efficiency, $Q_{hl, ref}$ is the reference thermal loss from the solar field at design, I_{bn} is the solar irradiation during the current time step, $I_{bn, des}$ is the design-point solar irradiation from the solar resource at the design input, and CF is the projected gross to net conversion factor.

By employing this comprehensive methodology, the study aims to provide a robust analysis of the proposed hybrid power plant, offering valuable insights into its economic viability, environmental benefits, and potential for sustainable energy generation. The combination of quantitative analysis, SAM simulation, and MCDM evaluation ensures an objective and detailed examination of the hybrid system, contributing to the advancement of renewable energy solutions in Saudi Arabia and beyond.

L. Economics of the Project

The economic analysis of the proposed hybrid power plant integrating CSP with an existing fossil fuel-based thermal power plant in Ar'Ar involves a comprehensive evaluation of the project's costs and financial viability. Table I presents a detailed breakdown of the costs considered for the modeling, derived from a market survey and cross-referenced with NREL's authoritative reference technical report on cost modeling of parabolic trough plants utilizing the SAM [16]. The cost estimation specifically focuses on the solar field and thermal storage sections of the parabolic trough system, as the power generation section is assumed to be already established and thus is not included in the analysis. Only operational costs are factored in, providing an accurate assessment of the economic aspects of the hybrid system. The core variables governing the project's economics are the Nominal Discount Rate (NDR), which is fixed at 8.14% and the presumed inflation rate, set at 2.5%. The project's anticipated lifetime is assumed to be 25 years, during which the financial performance and return on investment will be analyzed. These parameters play a crucial role in determining the LCOE and NPV of the hybrid power plant.

TABLE I. COST PARAMETERS OF A PARABOLIC TROUGH POWER PLANT

Parameter	Value	Parameter	Value
IRR	11%	DSCR	1.3
Target Year _{IRR}	20	Annual Interest Rate	7%
Price Escalation _{PPA}	1%/year	Solar Field	150
Analysis Period	25 years	HTF System	\$60/m ²
Inflation Rate	2.5%/year	Storage	\$65/kWe
NDR	8.14%/year	Others	\$120/kWe
Federal Income Tax	25%/year	Power Plant	\$50/kWe
Sales Tax	5%	Fuel	Variable

III. SITE SELECTION

Ar'Ar City has been meticulously chosen as the site for the proposed hybrid power plant. The decision to select Ar'Ar City is founded on a thorough geospatial analysis and site assessment, encompassing various factors that contribute to the location's suitability for the hybrid system.

A. Key Factors Influencing Site Selection

The existence of the Arar Gas Turbine Power Plant, a 470.2 MW thermal power project situated in Northern Borders, Saudi Arabia, played a pivotal role in the site selection process [31]. This power plant currently operates with oil as fuel and has been in commercial operation since 1985. It produces 519 Kg/MWh of CO₂ with a total of 212,657,000 kg [32]. Notably, the government's recent tender for the expansion of four units (25-30 MW each) at the power plant presents a unique opportunity to analyze the feasibility of integrating CSP technology into the existing infrastructure. This strategic alignment with the expansion project offers potential synergies and cost-effectiveness, making Ar'Ar an ideal location for the proposed hybrid power plant.

1) Grid Connectivity and Infrastructure

Ar'Ar has a well-established grid network, enabling efficient electricity transmission and distribution. The robust grid connectivity facilitates the seamless addition of the hybrid system to the existing infrastructure. This enhances the economic viability of the project and ensures a reliable electricity supply to the region.

2) Geographical and Climatic Factors

Geographically, Ar'Ar is positioned in the northern part of Saudi Arabia and serves as the capital of the Northern Border Province. Its strategic location near the border with Iraq and Jordan positions the city as a significant economic and transportation hub in the region. Ar'Ar has a desert climate common to the area, which is marked by hot summers and mild winters. The region receives abundant sunlight, with the average solar irradiance ranging from 4.5 to 7.6 kWh, making it well-suited for harnessing solar energy through CSP technology. Additionally, the city experiences moderate wind speeds of 7.3 to 9.4 miles per hour throughout the year, adding to its renewable energy potential.

3) Economic Landscape

Ar'Ar plays a vital role in agricultural activities, with crops like wheat, barley, and dates cultivated in the region. The city's agricultural sector also includes livestock farming. Industries

such as food processing, cement production, and construction contribute significantly to Ar'Ar's economic growth and development. These industries present promising opportunities for integrating renewable energy sources, including biomass for heat and power generation, further enhancing the city's overall sustainability.

4) Environmental Considerations

The site selection process considered environmental factors to minimize the project's impact on the local ecosystem and surroundings. Ar'Ar's potential for incorporating renewable energy solutions aligns with sustainability objectives, ensuring a balance between development needs and environmental conservation.

B. Energy Source Assessment

Energy source assessment is crucial for evaluating the renewable energy potential of the selected site. The primary focus is on solar power as the main renewable energy source for the proposed Hybrid Energy System (HES). To gather comprehensive data on solar and wind resources, the study relies on the National Aeronautics and Space Administration (NASA) database, a reputable source providing reliable meteorological information. Utilizing the NASA database, historical and real-time data on solar radiation levels and wind speed at Ar'Ar's geographical coordinates are obtained. These data are essential for accurately assessing the availability and variability of solar and wind sources throughout the year. It forms the basis for estimating the energy generation potential of CSP and wind turbines, the key components of the HES. By incorporating real-world data, we can conduct realistic simulations and in-depth analysis of the hybrid system's performance, considering the actual renewable energy potential at the site.

The simulation software used in this study (SAM), calculates the solar output using the global horizontal irradiance, which accounts for direct irradiance, diffused light, and reflected light. The solar radiation data collected from NASA's surface meteorology website were integrated into SAM, taking into account the location's coordinates. The study considers the average solar energy over 22 years to analyze seasonal variations in solar radiation and compute the global radiation incidence on the CSP [16]. The investigation shows that Ar'Ar witnessed a period of increased sunshine spanning over 3.5 months, starting on May 8 and ending on August 23. During this duration, the average irradiance remained above 7.6 kWh, particularly in June with an average daily solar radiation of 8.6 kWh. In winter, from November 3 to February 6, the average solar irradiance falls below 4.5 kWh. Notably, December emerges as the least radiant month, registering an average daily solar radiation of 3.5 kWh. The length of the day in Ar'Ar shows significant variation throughout the year. The shortest day is December 22 with a duration of about 10 hours, while the longest day is June 21 with about 14 hours of daylight. Additionally, on June 21 the earliest sunrise takes place (5:11 AM), whereas the latest sunrise occurs on January 9 (7:14 AM). Similarly, the earliest sunset occurs on December 3 (5:13 PM) and the latest sunset on July 1, 7:23 PM. Regarding the city's climate, Ar'Ar experiences a hot season starting on May 26 and ending on September 25. The average

temperature during that period is above 36 °C. July emerges as the hottest month (26-41 °C). Conversely, the cool season starts on November 25 and ends on March 2. The average temperature is normally below 20 °C. January is the coldest month (4 – 15 °C).

IV. CSP SYSTEM DESIGN

The selection of the parabolic trough model, SkyFuel Sky Trough, was made after a thorough evaluation of various CSP technologies. NREL's certification of this model as the most efficient technology in its category at a temperature of 350 °C makes it a compelling choice for the proposed hybrid energy system in Ar'Ar. Its high thermal efficiency of 73% ensures that a significant amount of solar energy is effectively captured and converted into usable heat. The absorber is a crucial component of the parabolic trough system, responsible for absorbing sunlight and converting it into thermal energy. Schott PTR80 was chosen as the absorber due to its superior performance and reliability. Its design allows for optimal absorption of solar radiation, maximizing the thermal output of the system. The specific properties of the PTR80 were carefully considered to ensure compatibility with the operating conditions of the CSP system.

One of the critical aspects of a CSP system is the HTF used to carry and transfer the captured thermal energy to the power generation unit. For this purpose, the HITEC solar salt was selected due to its exceptional characteristics that align with the system's requirements. The HITEC solar salt exhibits high specific heat (1.56 kJ/kg×C), allowing it to store and carry significant amounts of heat efficiently. Its low viscosity ensures smooth flow through the piping system, reducing energy losses during circulation. Moreover, the HITEC solar salt remains stable and chemically inert even under prolonged exposure to high temperatures, ensuring the longevity and reliability of the system. Table II provides detailed information about the collector, receiver, and HTF used in the parabolic CSP. The dimensions of the collector, including its aperture and assembly length, play a vital role in determining the amount of solar radiation captured and the overall performance of the system. Likewise, the receiver's design characteristics, such as the absorber tube's inner and outer diameter and total receiver losses, directly impact the efficiency of heat absorption and transfer.

TABLE II. CSP COMPONENT DETAILS

HTF	HITEC solar salt	Collector	SkyFuel Sky Trough
Single Loop Flow _{Max}	1 kg/sec	Reflective Aperture	656 m ²
Single Loop Flow _{Max}	12 kg/sec	Aperture Width	6 m
Field Flow Velocity _{Min}	0.268562 m/s	Assembly Collector Length	115 m
Field Flow Velocity _{Max}	3.74479 m/s	Water/wash	0.8 L/m ²
Receiver	Schott PTR80	Total Receiver Losses	211.35 W/m
Absorber Diameter _{Inner}	0.076 m	Washes/year	64
Absorber Diameter _{Outer}	0.08 m		

To analyze the potential impact of the CSP, various solar thermal capacities, ranging from 10 to 50 MW, were evaluated. This allows for a comprehensive analysis of the system's behavior and performance under different capacities, enabling more accurate predictions for larger-scale implementations. Table III presents the design of the different CSP capacities, revealing the relationship between the system capacity and key design parameters.

TABLE III. DESIGN OF DIFFERENT CSP CAPACITIES

Parameter	Values				
	10 MW	20 MW	30 MW	40 MW	50 MW
Capacity	10 MW	20 MW	30 MW	40 MW	50 MW
Actual No. of loops	17	33	49	65	82
Single loop aperture	5248 m ²	5248 m ²	5248 m ²	5248 m ²	5248 m ²
Reflective of total aperture area	89216 m ²	173184 m ²	257152 m ²	341120 m ²	430336 m ²
Field thermal output	56.1798 MWt	112.36 MWt	168.539 MWt	224.719 MWt	280.899 MWt
Total land area	77 Acres	150 Acres	222 Acres	295 Acres	372 Acres

The study considered 5 different capacity solar thermal systems, from 10 to 50 MW. As the capacity of the system increased, the number of loops required to achieve the desired thermal output also increased. For the 10 MW system, 17 loops were needed, while the 50 MW system required 82 loops. This relationship indicates that larger capacity systems demand a greater number of loops to efficiently capture and concentrate solar energy. As the system's capacity increased, the single loop aperture remained constant at 5248 m² for all capacity levels. However, the total aperture area, which represents the cumulative surface area of all loops in the system, increased significantly with higher capacity. For the 10 MW system, the total aperture area was 89,216 m², whereas for the 50 MW system, it expanded to 430,336 m². The total land area needed for the parabolic trough collectors and related infrastructure also increased. The 10 MW system demanded 77 acres of land, while the 50 MW system required a significantly larger land area of 372 acres. As expected, the thermal output increased proportionally with the system's capacity. The 10 MW system achieved a field thermal output of 56.1798 MWt, while the 50 MW system exhibited a substantial increase in thermal output, reaching 280.899 MWt. Furthermore, addressing the intermittency of solar energy availability is vital for ensuring a stable power supply. Hence, the study considers different thermal storage systems to store the excess thermal energy during sunny periods, which can then be utilized during peak load hours when solar energy may be limited. Table IV outlines the details of the different thermal storage systems analyzed in the study, including their storage volumes, thermal capacities, and estimated heat losses.

The increase in storage volume with higher system capacity can be attributed to the larger size and capacity of the thermal storage tanks. As the capacity of the hybrid energy system

increases from 10 to 50 MW, the number of thermal storage tanks and their dimensions scaled up accordingly. This allows for a greater volume of thermal energy storage, enabling the system to store more energy during periods of high solar irradiation. The rise in thermal capacity as the system capacity increases is a direct consequence of the larger size and number of thermal storage tanks in the system. With higher capacity systems, more thermal energy can be stored in the thermal storage tanks, resulting in increased thermal capacity. This enhanced thermal capacity ensures that the hybrid energy system can cater to the energy demands of Ar'Ar for longer durations, especially during peak load hours when solar energy generation may be insufficient. The relatively low estimated heat losses can be attributed to the careful selection of high-quality materials and design considerations in the thermal storage system. The use of advanced insulating materials and robust construction techniques minimizes heat losses from the thermal storage tanks.

higher CSP capacity leads to higher thermal capacity, allowing the hybrid energy system to store and supply more thermal energy to meet the city's energy demands.

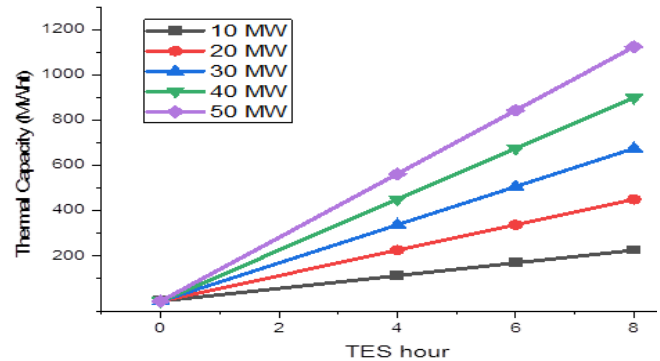


Fig. 1. Thermal capacity of the different storage systems.

TABLE IV. THERMAL STORAGE SYSTEM DETAILS

Full load hour of thermal storage	TES (0 hr)	TES (4 hr)	TES (6 hr)	TES (8 hr)
Storage Volume				
10MW	0 m ³	2196.5 m ³	3294.75 m ³	4392.99 m ³
20MW	0 m ³	4392.99 m ³	6589.49 m ³	8785.99 m ³
30MW	0 m ³	6589.49 m ³	9884.24 m ³	13179 m ³
40MW	0 m ³	8785.99 m ³	13179 m ³	17572 m ³
50MW	0 m ³	10982.5 m ³	16473.7 m ³	21965 m ³
Thermal Capacity				
10MW	0 MWh _t	112.36 MWh _t	168.539 MWh _t	224.719 MWh _t
20MW	0 MWh _t	224.719 MWh _t	337.079 MWh _t	449.438 MWh _t
30MW	0 MWh _t	337.079 MWh _t	505.618 MWh _t	674.157 MWh _t
40MW	0 MWh _t	449.438 MWh _t	674.157 MWh _t	898.876 MWh _t
50MW	0 MWh _t	561.798 MWh _t	842.697 MWh _t	1123.6 MWh _t
Estimated heat loss				
10MW	0 MW _t	0.098 MW _t	0.127 MW _t	0.152 MW _t
20MW	0 MW _t	0.152 MW _t	0.199 MW _t	0.243 MW _t
30MW	0 MW _t	0.199 MW _t	0.264 MW _t	0.324 MW _t
40MW	0 MW _t	0.243 MW _t	0.324 MW _t	0.399 MW _t
50MW	0 MW _t	0.284 MW _t	0.379 MW _t	0.471 MW _t

V. RESULTS AND DISCUSSION

A. Thermal Output

The results presented in Figure 1 show the thermal capacity of the different thermal storage systems for varying CSP capacities. The thermal capacity increases as the CSP capacity and thermal storage volume increase, demonstrating the potential benefits of increasing both parameters in the proposed hybrid energy system. As the CSP capacity increases from 10 MW to 50 MW, the thermal capacity of the system also increases significantly. This outcome is expected since a higher CSP capacity implies a larger solar energy generation capacity. With more solar energy being collected through the parabolic trough collectors, there is a greater amount of thermal energy available for storage in the thermal storage system. Therefore,

The thermal storage volume is another crucial factor influencing the thermal capacity of the system. By increasing the thermal storage volume, the system's capacity to act as a backup energy source also increases. This is particularly important for scenarios where solar energy generation is insufficient, such as during periods of low solar radiation or peak energy demand. A larger thermal storage volume enables the system to store surplus thermal energy during periods of high solar radiation and use it when solar energy generation is limited or unavailable. The results also demonstrate the significance of the full load hours of thermal storage TES (4 hr), TES (6 hr), and TES (8 hr) on the thermal capacity of the system. Longer full load hours correspond to higher thermal capacity values. For instance, with a 50 MW CSP capacity and the TES (8 hr) scenario, the thermal capacity reaches 1110 MWh_t, which is significantly higher than the thermal capacity of 500 MWh_t for TES (4 hr). This indicates that systems with longer full load hours can provide sustained and stable power generation during peak load periods or when the solar energy generation is low. The observed increase in thermal capacity with higher CSP capacity and thermal storage volume has practical implications for the proposed hybrid energy system in Ar'Ar. With a greater thermal capacity, the system becomes more reliable and capable of delivering a continuous power supply to the city, even during adverse weather conditions or fluctuations in solar energy availability. This enhanced energy reliability contributes to the overall stability and resilience of the city's power supply, reducing dependency on fossil fuel-based power generation and promoting sustainable and eco-friendly energy solutions.

The results presented in Figure 2 show the thermal losses in the different thermal storage systems with varying backup times and CSP capacities. As the backup time increases, the system stores the surplus thermal energy for longer periods without being utilized. This extended storage duration results in increased thermal losses due to various heat transfer mechanisms, such as thermal conduction, convection, and radiation. Longer backup times lead to higher losses, as indicated in Figure 2. While longer backup times enhance the system's ability to provide sustained power during periods of

low solar energy generation, it also means that more thermal energy is exposed to potential losses. The CSP capacity is another critical factor affecting thermal losses in the system. As the capacity increases, the storage volume will also increase. This means more thermal energy is available for storage, but it also translates to a larger surface area of the storage medium exposed to the surrounding environment. A larger storage volume means more surface area for heat exchange, which contributes to higher thermal losses. This is evident in the results presented in Figure 8, where increasing the storage volume results in higher thermal losses for all backup times and CSP capacities.

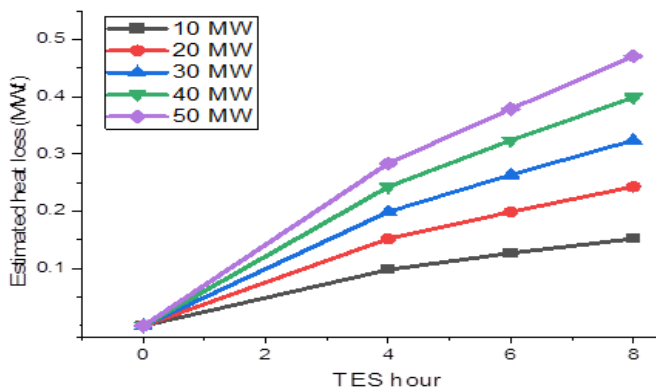


Fig. 2. Thermal losses in the storage systems.

To minimize thermal losses, strategies such as improving the insulation and thermal properties of the storage medium can be implemented. Using advanced thermal insulation materials and well-designed storage containers can reduce the heat transfer to the surroundings. Additionally, optimizing the operation and control of the thermal storage system can ensure that stored thermal energy is utilized efficiently without unnecessary losses.

B. Electrical Output

The capacity factor of the hybrid system, as shown in Figure 3, is a critical performance metric that indicates the efficiency and utilization of the system's installed capacity. The capacity factor is calculated as the ratio of the actual energy output (in MWh) to the maximum possible output if the system was operating at its rated capacity continuously throughout the year. The capacity factor of the solar thermal parabolic trough systems without thermal energy storage (TES (0 hr)) is approximately 31-32% due to the limited availability of sunlight during the day cycle. Solar energy can be harnessed effectively only during periods of sufficient irradiance, which is typically around 7 hours per day. Therefore, the system operates at its full capacity only for this limited duration, resulting in a relatively lower capacity factor. Incorporating TES systems significantly impacts the capacity factor of the hybrid system. With the addition of thermal energy storage, the plant can store the excess thermal heat produced during periods of high solar irradiance and utilize it when the sun is not available, extending the operation time of the plant beyond the sunlight hours.

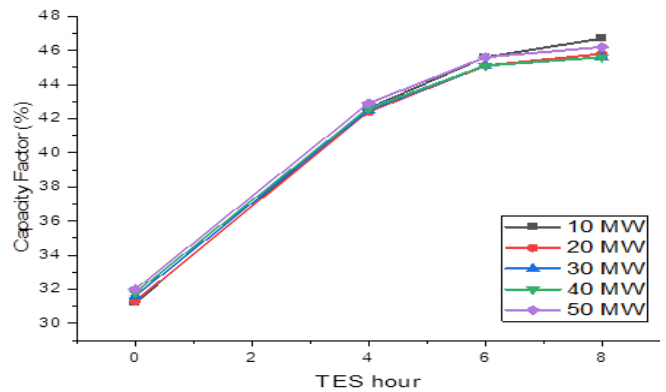


Fig. 3. Capacity factor of the different parabolic trough systems.

As shown in Figure 3, increasing the CSP capacity has little impact on the capacity factor but with the introduction of TES systems (TES (4 hr), TES (6 hr), and TES (8 hr)), the capacity factor of the hybrid system increases. The more extensive the thermal storage capacity (higher backup times), the more the plant can operate and generate power beyond the available sunlight hours. The thermal storage capability allows the system to operate at or near its full capacity even after the sun has set or during periods of low solar irradiance. This ability to provide electricity continuously, despite fluctuations in solar availability, leads to higher capacity factors. Therefore, increasing the thermal storage capacity can significantly improve the system's capacity factor, ultimately enhancing its overall performance and economic viability.

The yearly electrical output of the different parabolic trough capacities, as presented in Figure 4, provides valuable insights into the performance of the hybrid system under varying CSP capacities and TES durations. As expected, the electrical power output of the hybrid system increases with the CSP capacity. Larger capacity systems, such as the 40 MW and 50 MW configurations, capture more heat from the field, resulting in higher power generation. This relationship is due to the higher number of loops and larger apertures, which allow for more efficient heat collection and conversion into electricity.

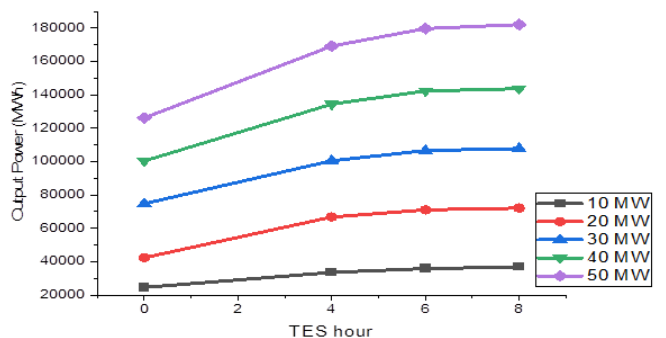


Fig. 4. Electrical output from the different capacities.

The presence of TES in the hybrid system enhances its performance by allowing the stored thermal energy to be utilized during periods of low solar irradiance or after sunset. However, the influence of thermal storage on the power output

varies with the CSP capacity. For lower-capacity systems, such as the 10 MW configuration, increasing the thermal storage backup time has a limited effect on power output, because the overall energy captured from the field is relatively lower, and the system may already be operating close to its maximum capacity without significant excess heat for storage. As a result, the additional thermal energy stored has a minimal impact on overall power generation. In contrast, for larger capacity systems (40 MW and 50 MW), increasing the thermal storage backup time results in a substantial rise in power output. These larger systems have higher energy capture capabilities, and the additional thermal energy stored allows for continuous power generation even during extended periods of low solar irradiance. The performance of the system becomes saturated after a certain thermal storage backup time. For example, with the 40 MW and 50 MW systems, the power output reaches its peak at a 6-hour thermal storage backup, and further increasing the backup time has a diminishing impact on power output. This suggests that the system's design and operational parameters should be optimized to achieve the best balance between thermal storage and power generation. In this study, this has been done through the MCDM technique.

C. Economic Analysis

The net present cost analysis of the parabolic trough system, as presented in Figure 5, provides valuable insights into the economic implications of varying system capacities and the incorporation of thermal storage. The findings show that as the capacity of the CSP increases, there is a corresponding rise in the net present cost. This relationship can be attributed to several factors including land area, more components, and size. Larger capacity systems require more land to accommodate a higher number of loops and a larger aperture area. Acquiring and preparing larger land areas contribute to the overall capital cost of the system. Higher capacity systems necessitate more components, such as mirrors, absorber tubes, and support structures, resulting in higher manufacturing and installation costs. With increased capacity, the physical size of the parabolic trough system also grows, leading to higher material and construction expenses.

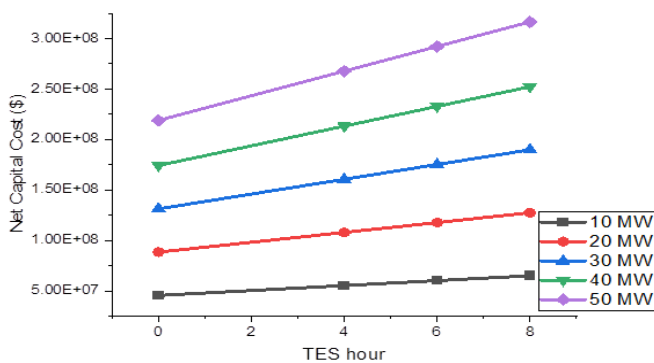


Fig. 5. Net capital cost of the CSP.

The incorporation of TES into the parabolic trough system introduces additional costs. This is primarily due to the need for storage tanks, additional molten salt, and heaters to store and maintain thermal energy for extended periods. As the

thermal storage backup time increases, more storage volume and salt are required, resulting in further cost increments. The 10 MW system exhibits the lowest net present cost, primarily because it requires less land, and fewer components, and has a smaller physical footprint than the higher capacity systems. Conversely, the 50 MW system shows the highest net present cost due to its larger size and increased material requirements. The cost difference between the 10 MW and 50 MW systems can be substantial, highlighting the economic advantages of considering lower capacity configurations for smaller-scale applications.

The results indicate that the net present cost increases as the thermal storage backup time increases. While thermal storage enhances the system's performance and enables continuous power generation, it comes with additional capital expenses. It is crucial to evaluate the trade-offs between increased capital costs and improved power generation reliability when deciding on the optimal thermal storage duration. For project developers and stakeholders, finding the optimal balance between capacity and thermal storage is essential to achieve cost-effective system designs. In this study, this has been done through the MCDM.

The cost of electricity generated by the parabolic trough system, as presented in Figure 6, provides valuable insights into the economic feasibility and efficiency of the system at different capacity levels and with varying thermal energy storage durations. At the outset, the cost of electricity production ranges from 14.5 to 15.5 cents per kilowatt-hour (¢/kWh). This cost reflects the initial capital investments, operational expenses, and solar thermal capacity of the parabolic trough system. As expected, larger capacity systems generally have lower costs of electricity generation compared to smaller systems due to economies of scale. This is a significant advantage of larger capacity systems, as they can harness more solar energy, resulting in a higher thermal output. The decrease in cost can be attributed to the spreading of the fixed capital and operational costs over a larger energy generation capacity, leading to a reduced cost per unit of the produced electricity. However, even the initial costs of electricity production are competitive with conventional power sources, making the parabolic trough system a viable renewable energy option.

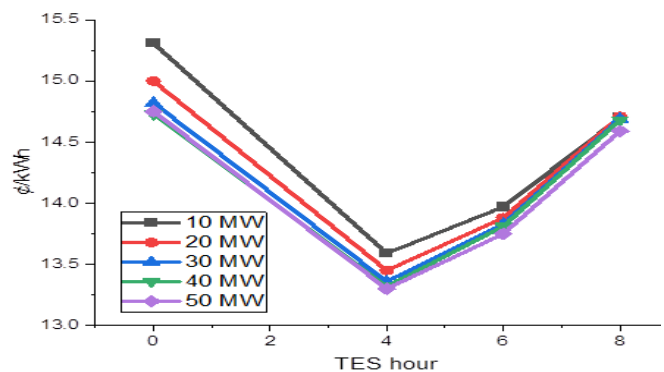


Fig. 6. Cost of electricity produced by the CSP.

The addition of 4-hour thermal storage to the system results in a cost reduction of approximately 2 ¢/kWh. TES allows the system to save the excess thermal energy during peak sunlight time and utilize it during times of lower solar irradiance or after sunset. This enables a more consistent and reliable electricity output, reducing the reliance on immediate solar availability and, consequently, the cost of electricity production. However, the results show that further increase in thermal storage beyond 4 hours leads to an increase in the cost of electricity. This phenomenon can be attributed to diminishing returns on investment. While longer thermal storage durations provide more backup energy, the additional capital and operational costs associated with larger storage volumes and extended thermal storage times may outweigh the benefits. The competitive cost of electricity production from the parabolic trough system, particularly at larger capacity levels with the 4-hour thermal storage, positions it as a promising contender in the energy market. As the cost of conventional fossil-fuel-based electricity generation continues to rise and environmental concerns drive the demand for sustainable energy alternatives, the parabolic trough system's cost-effectiveness can attract investors and utilities seeking cleaner and economically viable energy solutions.

D. MCDM Selection

The performance of the CSP systems with varying TES configurations exhibited diverse outcomes. As the TES capacity increased, there was a notable improvement in both thermal and electrical outputs, which are advantageous as they allow for higher energy capture and utilization. However, it was also observed that increasing the TES capacity led to higher losses in the system, as energy was stored for longer periods without being fully utilized. These losses arise from thermal conduction, convection, and radiation during the storage process. Additionally, the incorporation of TES resulted in higher Net Present Cost (NPC) and Cost of Electricity (COE) due to the need for additional storage tanks, molten salt, and heaters, which incur additional capital and operational expenses. To strike an optimal balance between the benefits and drawbacks of different TES capacities, the MCDM method was employed (Pohekar & Ramachandran, 2004). MCDM is a powerful decision-making technique that evaluates multiple solutions based on various predefined criteria and considerations. It allows for a comprehensive and systematic evaluation of renewable energy systems, considering both qualitative and quantitative aspects. In the context of the CSP system, MCDM considered factors such as thermal and electrical outputs, losses, NPC, and COE, among others. The identified MCDM criteria are shown in Table V.

TABLE V. SELECTED CRITERIA FOR MCDM

Criteria	Sub-Criteria		Unit
Thermal	Thermal Capacity	C1	MWh
	Thermal Losses	C2	MWh
Electrical	Capacity Factor	C3	%
	Output Power	C4	MWh
Economical	NPC	C5	\$
	COE	C6	¢/kWh

The AHP-SAW combination [13] was used in the MCDM technique applied in this study. The Analytical Hierarchy Process (AHP) was used to assign appropriate weights to each criterion [22]. This step was crucial to ensure that the decision-making process accurately captured the significance of each criterion in the context of the CSP system's performance. Data analysis and evaluation were carried out using the Simple Additive Weightage (SAW) method [7]. The SAW method calculates the weighted sum of performance evaluations for each alternative across all attributes. The SAW utilizes predefined values and preference weights, leading to more precise selection. By employing a comparison decision matrix, direct comparisons between each criterion and its counterpart were made, facilitating the identification of the most influential criteria. The pairwise comparison matrix utilized a scale from 1 to 9, representing the relative importance of each criterion in relation to others. The square matrix $A = m \times m$ (where m represents the number of criteria) was used to create the pairwise comparison matrix. The entry value in the comparison matrix, a_{ij} , indicates the comparison value between the i th (row) criterion and the j th (column) criterion. The values of the comparison matrix are provided for all criteria, as shown in Table VI, and were formulated through (11) to enable direct evaluations between each criterion and its corresponding counterpart. These values were derived after carrying out a literature review of MCDM being applied to solar energy. Through this analysis, the relative importance of each criterion was identified, and corresponding numerical values were assigned.

$$A = (a_{ij}) \tag{11}$$

$$a_{ij} = \frac{1}{a_{ji}} \text{ if } i \neq j, \quad \text{else if } i = j, a_{ij} = 1$$

TABLE VI. PAIRWISE VALUES OF THE COMPARISON MATRIX.

	C1	C2	C3	C4	C5	C6
C1	1	0.25	2	2	2	2
C2	4	1	3	2	2	6
C3	0.5	0.33	1	0.5	2	2
C4	0.5	0.5	2	1	2	3
C5	0.5	0.5	0.5	0.5	1	3
C6	0.5	0.17	0.5	0.33	0.33	1
SUM	8.65	3.82	10.25	7.35	10.42	19.02

TABLE VII. NORMALIZED PAIRWISE MATRIX

	C1	C2	C3	C4	C5	C6
C1	0.116	0.065	0.195	0.272	0.192	0.105
C2	0.462	0.262	0.293	0.272	0.192	0.315
C3	0.058	0.086	0.098	0.068	0.192	0.105
C4	0.058	0.131	0.195	0.136	0.192	0.158
C5	0.058	0.131	0.049	0.068	0.096	0.158
C6	0.058	0.045	0.049	0.045	0.032	0.053

In the next step, it is necessary to normalize each value in the pairwise comparison matrix by dividing it by the sum of the values within the corresponding column. This normalization process ensures the creation of a normalized pairwise comparison matrix. The value of the normalized matrix is calculated by:

$$a_{ij} = \frac{a_{ij}}{\sum_{l=1}^m a_{il}} \tag{12}$$

To obtain the overall weight vector, the final step involves averaging each row of the matrix presented in Table VIII. This averaging process is carried out by:

$$w_i = \sum_{l=1}^m a_{il} \tag{13}$$

TABLE VIII. OVERALL WEIGHT OF EACH CRITERION

C1	C2	C3	C4	C5	C6
0.159	0.146	0.149	0.184	0.153	0.208

The resulting priority vector was verified using the consistency verification process to validate the reliability of the decision-making matrix. The Consistency Ratio (CR) obtained, which was below 10% (8.8%), demonstrated the credibility and accuracy of the priority vector, thus ensuring the robustness of the MCDM analysis.

The multi-criteria utility function (U) played a vital role in evaluating the alternative TES configurations. By consolidating diverse criteria into a single utility value, the utility function enabled effective comparison and ranking of the options. The utility function assigned weights to each criterion based on their relative importance, as determined by the AHP technique. Through the application of the utility function, the performance of each alternative across different criteria was transformed into a single utility value, facilitating comprehensive and well-informed comparisons. The calculation of the multi-criteria utility function, incorporating the weights of all the criteria, is provided in (14):

$$U = 0.159 \times [C1] + 0.146 \times [C2] + 0.149 \times [C3] + 0.184 \times [C4] + 0.153 \times [C5] + 0.208 \times [C6] \tag{14}$$

First, the MCDM was applied to the 10 MW system. The final step of score and rank is calculated by ranking the alternatives from the sum of decision matrix multiplication by weights using (14). The application of MCD on all the CSP capacity systems provided valuable insights into the optimal TES configuration. Table IX illustrates the rankings obtained, where the 4-hour TES system consistently ranked 1st among the CSP capacities, indicating that this system configuration is most aligned with the identified criteria and is well-suited for addressing the technical and economic aspects of the project. Following closely in second place is the 6-hour TES configuration, whereas the 0-hour configuration obtained the lowest score.

TABLE IX. MCDM RANKING OF THE CSP SYSTEMS

System	Rank				
	10MW	20MW	30MW	40MW	50MW
0hrs	4	4	4	4	4
4hrs	1	1	1	1	1
6hrs	2	2	2	3	3
8hrs	3	3	3	2	2

The primary reason for the 4-hour TES system consistently ranking 1st is its significantly lower COE compared to the other TES configurations. The COE is a critical metric in evaluating the economic viability and competitiveness of renewable energy systems. With a 4-hour TES system, the CSP

plant benefits from efficient energy storage, enabling it to generate and deliver electricity at a lower cost. As a result, the cost of electricity production is minimized, making the CSP plant more economically feasible and attractive to investors and consumers. Additionally, another contributing factor to the preference for the 4-hour TES system is that the output power achieves saturation beyond the 4-hour storage duration. Beyond this point, increasing the TES capacity does not yield a proportional increase in output power. The system reaches a point of diminishing returns, where the benefits of additional thermal storage capacity are outweighed by the increased costs and losses associated with larger storage volumes. As TES capacity increased beyond 4 hours, the NPC of the CSP system also increases significantly. The NPC considers the total capital costs and operational expenses over the lifetime of the system, discounted to their present value. Larger TES systems require more storage tanks, additional molten salt, and heaters, leading to higher initial investment and maintenance costs. This affects the overall economic feasibility of the CSP plant, as higher NPC values translate to higher electricity tariffs. Furthermore, increasing the TES capacity also leads to higher thermal losses. As the energy is stored for longer periods without being utilized, there is an increased risk of heat losses due to thermal conduction, convection, and radiation. These losses reduce the overall efficiency of the CSP system and result in a decrease in the amount of electricity that can be generated from the captured heat.

E. Fossil Fuel Compensation by CSP with 4-Hour TES

Figure 7 presents the field thermal output of the various parabolic trough capacities with the 4-hour TES, and a clear trend emerges as the system's capacity increases. The field thermal output rises rapidly with higher system capacities. This is because as the capacity of the CSP system increases, more parabolic trough loops are added to the design, which directly impacts the total reflective aperture area. The larger the aperture area, the more sun light can be captured and used as thermal energy. This phenomenon leads to a significant boost in the field thermal output. Notably, the 40 MW (250 MWt) and 50 MW (280 MWt) systems demonstrate impressive thermal energy generation, producing over 200 MWt of thermal energy when equipped with a 4-hour TES system. This is a substantial amount of thermal energy, and it has practical implications in the context of hybrid systems that include fossil-fuel burners. In contrast, the 10 MW system, while still a significant renewable energy source, produces a lower field thermal output of 60 MWt due to the smaller aperture area and fewer parabolic trough loops in the system. While it may be suitable for specific applications, it might not provide enough thermal energy to sustain a hybrid system continuously without additional backup sources.

The results presented in Figure 8 highlight the significant advantages of integrating solar thermal energy as a heat source to the power plant's boiler in the hybrid system. By doing so, the consumption of hydro carbon fuels in the power generation process can be substantially reduced. One key observation from the data is that as the capacity of the parabolic trough system increases, the amount of heat input to the boiler also increases. This, in turn, results in a proportional reduction in the

consumption of fossil fuels. The reason behind this trend lies in the fact that larger capacity parabolic trough systems capture and convert more solar energy into thermal energy. Consequently, a greater amount of thermal energy is supplied to the hybrid system, thereby reducing the reliance on fossil fuels to meet the required heat input in the boiler.

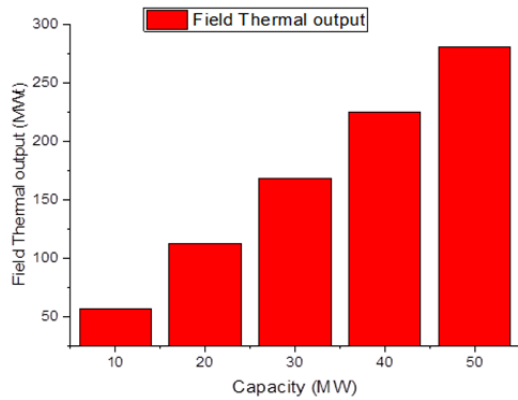


Fig. 7. Field thermal output with a 4-hour TES system.

For instance, the 10 MW CSP with 4 hours of TES enables the saving of approximately 18.84 tons of coal per hour. As the capacity of the parabolic trough system is increased to 50 MW, the coal savings rise to an impressive 96 tons per hour, demonstrating that the larger the capacity of the parabolic trough system, the higher the reduction in coal consumption, resulting in significant cost savings and environmental benefits. Similarly, the hybrid system's integration with solar thermal energy also leads to substantial savings in oil and gas consumption. As the capacity of the parabolic trough system increases, the amount of oil and gas saved per hour increases proportionally. For example, the 50 MW parabolic trough system with 4 hours of TES can save approximately 48 barrels of oil and 400,000 ft³ of gas per hour. These results have profound implications for the energy industry and the transition towards cleaner and more sustainable energy sources. By incorporating solar thermal energy into the hybrid system, the dependence on fossil fuels is significantly reduced, leading to a more environmentally friendly power generation process. The reduction in hydro carbon fuel consumption not only helps decrease CO₂ emissions and combat climate change, but also offers economic advantages through cost savings.

The data presented in Figure 9 highlight the substantial cost savings achieved by implementing the solar thermal parabolic trough system in the hybrid power plant. As the capacity of the parabolic trough system increases, the cost savings from reducing fossil fuel consumption also increase, demonstrating the economic viability and benefits of larger-scale renewable energy integration. One key factor influencing the cost savings is the type of fuel used in the power generation process. The data indicate that oil is the most expensive fuel, followed by coal and gas, with gas being the cheapest. Consequently, the largest savings are done by decreasing oil consumption, while the least savings are done by decreasing gas consumption.

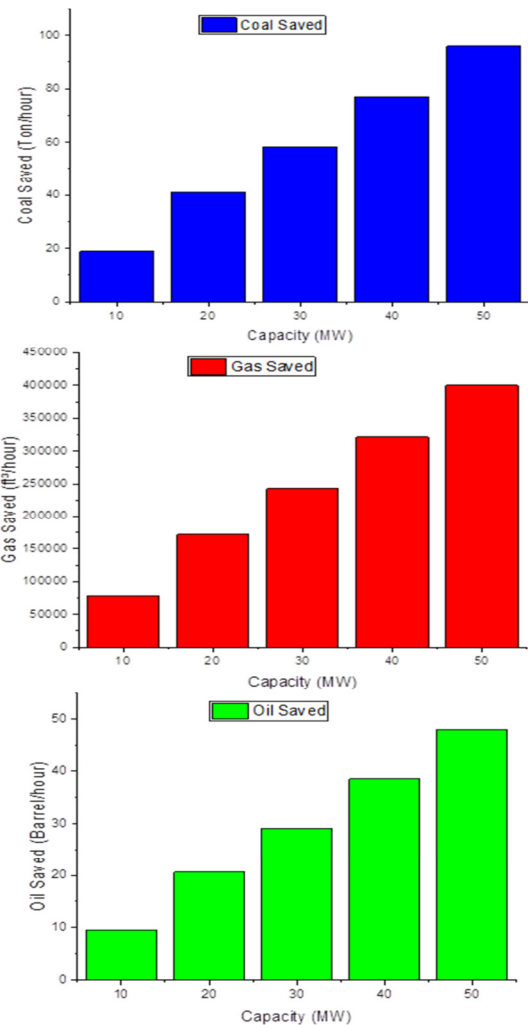


Fig. 8. Reduction in fuel consumption with the 4-hour TES system.

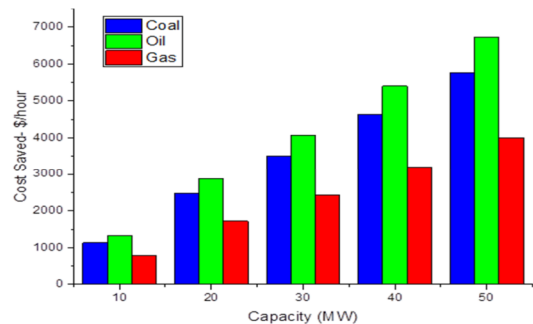


Fig. 9. Fossil fuel cost saving with the 4-hour TES system.

For instance, the 10 MW CSP with the 4-hour TES achieves cost savings of approximately 1130.4 \$/hour from reduced coal consumption, 1318.8 \$/hour from reduced oil consumption, and 785 \$/hour from reduced gas consumption. As the capacity of the parabolic trough system increases to 50 MW, the cost savings rise significantly to 5760.00 \$/hour from reduced coal consumption, 6720 \$/hour from reduced oil consumption, and 4000 \$/hour from reduced gas consumption.

These findings underscore the economic advantages of incorporating solar thermal energy into the hybrid power plant. By displacing costly fossil fuels with renewable energy, the overall operating costs of the power plant are significantly reduced. This translates to lower electricity production costs and, in turn, benefits consumers by potentially lowering electricity prices.

The results presented in Figure 10 demonstrate the significant environmental benefits of integrating CSP into the hybrid system. Fossil fuel consumption, is a major source of carbon dioxide (CO₂) emissions, which contributes to climate change and environmental degradation. By utilizing solar thermal energy as a clean and renewable alternative, the system can effectively reduce its reliance on fossil fuels and subsequently decrease CO₂ emissions, mitigating the negative impact on the environment. As the capacity of the parabolic trough system increases, the reduction in CO₂ emissions becomes more pronounced, indicating the potential for larger-scale renewable energy integration to make a more substantial contribution to climate change mitigation. The reduction in CO₂ emissions is most significant for coal consumption, as coal has the highest carbon content among the three fossil fuels considered. For instance, the 10 MW CSP with 4-hour TES reduces CO₂ emissions by approximately 18,340.112 kg/hour from coal consumption, 14,004.4 kg/hour from oil consumption, and 6,990.896 kg/hour from gas consumption. As the capacity of the parabolic trough system increases to 50 MW, the reduction in CO₂ emissions rises significantly to 93,452.8 kg/hour from coal consumption, 71,360 kg/hour from oil consumption, and 35,622.4 kg/hour from gas consumption. It is worth noting that these reductions in CO₂ emissions have substantial environmental implications. By decreasing the emission of CO₂, solar thermal integration helps combat climate change and contributes to the global effort to limit temperature rise and its associated adverse effects.

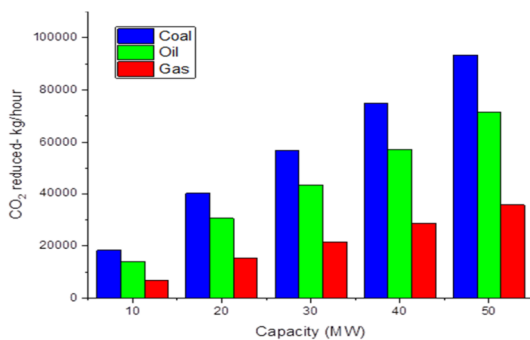


Fig. 10. Reduction in CO₂ emissions with the 4-hour TES system.

Figure 11 provides valuable insights into the financial performance of the parabolic trough system with the 4-hour TES over its operational lifetime. The graph showcases the payback period, the point at which the initial investment in the system is recovered, and the subsequent revenue generation over time. It is a critical metric that assesses the duration it takes for the system's cumulative revenue to equal the initial investment cost. As shown in the graph, the payback period for the CSP is approximately 12 years. This means that after 12

years of operation, the system has generated enough revenue to cover the initial capital expenditure, and from that point forward, it begins to generate net positive revenue.

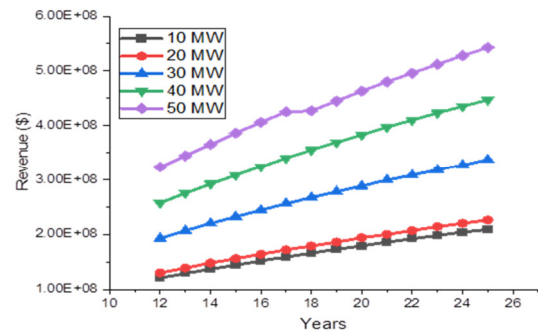


Fig. 11. Revenue created by the systems with 4-hour TES.

The size of the parabolic trough system plays a vital role in determining its revenue generation. Larger systems with higher capacities have a greater electric power output, which translates to higher revenue potential. As depicted in the graph, the 50 MW system, being the largest in capacity, generates significantly more revenue compared to the 10 MW system. The 10 MW system reaches a revenue of approximately \$120 million by the end of the 12-year payback period. Over the entire project life, the revenue for the 10 MW system rises to \$210 million. In contrast, the 50 MW system, with its greater electric power output, achieves a revenue of approximately \$325 million during the 12-year payback period. Over the entire project life, the revenue for the 50 MW system rises to the impressive \$545 million. This substantial revenue generation demonstrates the financial viability of larger capacity parabolic trough systems and their ability to deliver long-term economic benefits. The revenue generation for the parabolic trough system after the payback period is particularly significant as it contributes to the overall profitability and financial sustainability of the project. As the revenue generation continues to exceed operational costs, the system generates positive cash flow, allowing for potential reinvestment, debt reduction, or shareholder returns. The revenue generation is directly linked to the system's electric power output and its ability to supply energy to the grid or end-users. Therefore, ensuring the optimal performance and efficiency of the parabolic trough system is essential to maximize revenue generation throughout its operational life.

Figure 12 provides crucial insights into the long-term performance of the parabolic trough systems, considering the inevitable impact of environmental factors on their efficiency and effectiveness. As parabolic troughs are continuously exposed to various environmental elements, wear and tear occur over time, leading to degradation in their overall performance. The environmental factors that contribute to the degradation of the system's performance include humidity, UV radiation, loss of reflector shine, reduction of absorber's absorption capacity, loss of HTF storage capability, rust formation, and pollution. Each of these factors can have a cumulative effect on the system's components, potentially leading to diminished energy capture and conversion efficiency.

As shown in the results, all parabolic trough systems, regardless of their capacity, experience a decline in performance over time. This degradation is a natural consequence of the prolonged exposure to harsh environmental conditions. However, the effect is more pronounced in larger systems compared to smaller ones. The larger systems have a higher number of components and a larger surface area exposed to environmental factors, making them more susceptible to wear and deterioration. Consequently, the 50 MW system experiences a more significant reduction in production compared to the 10 MW system. By the end of the project life, the 50 MW system's energy production decreased from 180 million kWh to 69 million kWh. In contrast, the 10 MW system's energy production reduces from 3.5 million kWh to 1.5 million kWh. The implications of such performance degradation are significant, both economically and environmentally. From an economic perspective, the reduced energy production leads to lower revenue generation, potentially affecting the financial viability of the project. Furthermore, the decreased efficiency may necessitate maintenance and refurbishment efforts to restore the system's performance, incurring additional costs. From an environmental standpoint, the decline in energy production translates to a decreased contribution of renewable energy to the grid, potentially leading to a higher reliance on fossil fuel-based power generation during periods of reduced solar energy capture. This, in turn, could result in increased greenhouse gas emissions and environmental impacts. To mitigate the effects of performance degradation, regular maintenance, and monitoring of the parabolic trough systems are essential. Implementing proper cleaning protocols, replacing degraded components, and optimizing the system's operation can help slow down the decline in performance and extend the system's useful life. Moreover, advancements in materials and coatings that enhance the system's durability and resistance to environmental factors can further improve the long-term performance of parabolic troughs.

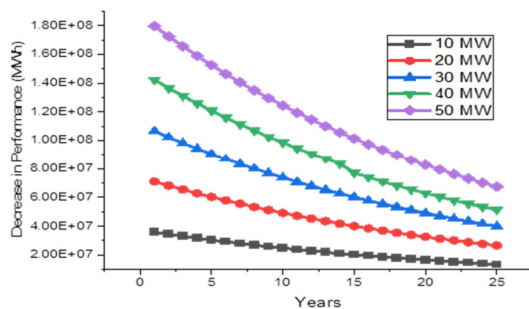


Fig. 12. The decrease in system performance.

VI. CONCLUSION

This study focuses on the design, performance analysis, and economic evaluation of solar thermal parabolic trough systems with different capacities and Thermal Energy Storage (TES) durations. Through a comprehensive investigation and analysis of various parameters, we gained valuable insights into the feasibility and effectiveness of these systems in harnessing solar energy for power generation. The results and discussion shed light on the key factors that influence the system's

performance, economic viability, and environmental impact. The findings reveal that increasing the capacity of the parabolic trough system results in higher thermal output and electrical generation. The thermal capacity increases as the CSP capacity increases, with the 50 MW system achieving a thermal output of 280.899 MWt. This demonstrates that larger systems can capture more heat from the sun, enhancing their overall energy output. Furthermore, the incorporation of TES in the system proves to be beneficial in extending the operation time of the plant, particularly after sunset. The capacity factor of the hybrid system increases with the integration of TES. The 4-hour TES provides the best trade-off between thermal capacity and losses, resulting in an optimal cost of electricity. The economic evaluation reveals that larger capacity systems incur higher net capital costs, but they also generate significantly more revenue over time. Despite higher initial investments, larger systems achieve larger payback and revenue generation in the same timeframe, making them financially attractive in the long run. Moreover, the integration of solar thermal energy into the hybrid power plant significantly reduces the consumption of fossil fuels. This reduction leads to cost savings and, more importantly, helps mitigate CO₂ emissions. The 50 MW system saves approximately 96 tons/hour of coal, 48 barrels/hour of oil, and 400,000 ft³/hour of gas. This reduction in CO₂ emissions is crucial in contributing to environmental sustainability and combating climate change. However, it is important to consider the performance degradation of the parabolic trough systems over time. Environmental factors, such as humidity, UV radiation, and pollution, lead to wear and tear, resulting in reduced energy production. Regular maintenance and technological advancements are essential in addressing this issue and maximizing the system's operational life.

In conclusion, the results presented and discussed in this paper demonstrate the promising potential of solar thermal parabolic trough systems in meeting the energy demands sustainably. Larger capacity systems with 4-hour TES prove to be economically viable, environmentally beneficial, and capable of achieving payback in a relatively short period. These systems offer a reliable and efficient means of generating renewable energy while reducing dependence on fossil fuels and reducing CO₂ emissions. As the world strives towards a greener and more sustainable future, the findings from this study provide valuable insights and guide decision-makers in harnessing the power of solar energy to meet the challenges of the 21st century.

ACKNOWLEDGMENT

The authors gratefully thank the Prince Faisal bin Khalid bin Sultan Research Chair in Renewable Energy Studies and Applications (PFCRE) at Northern Border University for their support and assistance.

REFERENCES

- [1] A. Gani, "Fossil fuel energy and environmental performance in an extended STIRPAT model," *Journal of Cleaner Production*, vol. 297, May 2021, Art. no. 126526, <https://doi.org/10.1016/j.jclepro.2021.126526>.
- [2] Y. Sribna, O. Trokhymets, I. Nosatov, and I. Kriukova, "The globalization of the world coal market – contradictions and trends," *E3S*

- Web of Conferences, vol. 123, 2019, Art. no. 01044, <https://doi.org/10.1051/e3sconf/201912301044>.
- [3] M. A. Lange, "Impacts of Climate Change on the Eastern Mediterranean and the Middle East and North Africa Region and the Water-Energy Nexus," *Atmosphere*, vol. 10, no. 8, Aug. 2019, Art. no. 455, <https://doi.org/10.3390/atmos10080455>.
- [4] M. A. Gonzalez-Salazar, T. Kirsten, and L. Prchlik, "Review of the operational flexibility and emissions of gas- and coal-fired power plants in a future with growing renewables," *Renewable and Sustainable Energy Reviews*, vol. 82, pp. 1497–1513, Feb. 2018, <https://doi.org/10.1016/j.rser.2017.05.278>.
- [5] D. Gielen, F. Boshell, D. Saygin, M. D. Bazilian, N. Wagner, and R. Gorini, "The role of renewable energy in the global energy transformation," *Energy Strategy Reviews*, vol. 24, pp. 38–50, Apr. 2019, <https://doi.org/10.1016/j.esr.2019.01.006>.
- [6] E. A. Al-Ammar, N. H. Malik, and M. Usman, "Application of using Hybrid Renewable Energy in Saudi Arabia," *Engineering, Technology & Applied Science Research*, vol. 1, no. 4, pp. 84–89, Aug. 2011, <https://doi.org/10.48084/etasr.33>.
- [7] A. Ibrahim and R. A. Surya, "The Implementation of Simple Additive Weighting (SAW) Method in Decision Support System for the Best School Selection in Jambi," *Journal of Physics: Conference Series*, vol. 1338, no. 1, Jul. 2019, Art. no. 012054, <https://doi.org/10.1088/1742-6596/1338/1/012054>.
- [8] M. A. Baseer, S. Rehman, J. P. Meyer, and Md. M. Alam, "GIS-based site suitability analysis for wind farm development in Saudi Arabia," *Energy*, vol. 141, pp. 1166–1176, Dec. 2017, <https://doi.org/10.1016/j.energy.2017.10.016>.
- [9] A. H. Almasoud and H. M. Gandayh, "Future of solar energy in Saudi Arabia," *Journal of King Saud University - Engineering Sciences*, vol. 27, no. 2, pp. 153–157, Jul. 2015, <https://doi.org/10.1016/j.jksues.2014.03.007>.
- [10] Y. H. A. Amran, Y. H. M. Amran, R. Alyousef, and H. Alabduljabbar, "Renewable and sustainable energy production in Saudi Arabia according to Saudi Vision 2030: Current status and future prospects," *Journal of Cleaner Production*, vol. 247, Feb. 2020, Art. no. 119602, <https://doi.org/10.1016/j.jclepro.2019.119602>.
- [11] I. Tlili, "Renewable energy in Saudi Arabia: current status and future potentials," *Environment, Development and Sustainability*, vol. 17, no. 4, pp. 859–886, Aug. 2015, <https://doi.org/10.1007/s10668-014-9579-9>.
- [12] O. Alnathier, "The potential contribution of renewable energy to electricity supply in Saudi Arabia," *Energy Policy*, vol. 33, no. 18, pp. 2298–2312, Dec. 2005, <https://doi.org/10.1016/j.enpol.2003.12.013>.
- [13] A. Alanazi and M. Alanazi, "Multicriteria Decision-Making for Evaluating Solar Energy Source of Saudi Arabia," *Sustainability*, vol. 15, no. 13, Jan. 2023, Art. no. 10228, <https://doi.org/10.3390/su151310228>.
- [14] M. M. A. Khan, M. Asif, and E. Stach, "Rooftop PV Potential in the Residential Sector of the Kingdom of Saudi Arabia," *Buildings*, vol. 7, no. 2, Jun. 2017, Art. no. 46, <https://doi.org/10.3390/buildings7020046>.
- [15] S. T. Jan and M. Noman, "Influence of absorption, energy band alignment, electric field, recombination, layer thickness, doping concentration, temperature, reflection and defect densities on MAGE13 perovskite solar cells with Kesterite HTLs," *Physica Scripta*, vol. 97, no. 12, Aug. 2022, Art. no. 125007, <https://doi.org/10.1088/1402-4896/ac9e7f>.
- [16] D. Bishoyi and K. Sudhakar, "Modeling and performance simulation of 100MW PTC based solar thermal power plant in Udaipur India," *Case Studies in Thermal Engineering*, vol. 10, pp. 216–226, Sep. 2017, <https://doi.org/10.1016/j.csite.2017.05.005>.
- [17] A. Boretti, "Cost and production of solar thermal and solar photovoltaics power plants in the United States," *Renewable Energy Focus*, vol. 26, pp. 93–99, Sep. 2018, <https://doi.org/10.1016/j.ref.2018.07.002>.
- [18] R. P. Praveen, M. Abdul Baseer, A. B. Awan, and M. Zubair, "Performance Analysis and Optimization of a Parabolic Trough Solar Power Plant in the Middle East Region," *Energies*, vol. 11, no. 4, Apr. 2018, Art. no. 741, <https://doi.org/10.3390/en11040741>.
- [19] S. Tariq Jan and M. Noman, "Influence of layer thickness, defect density, doping concentration, interface defects, work function, working temperature and reflecting coating on lead-free perovskite solar cell," *Solar Energy*, vol. 237, pp. 29–43, May 2022, <https://doi.org/10.1016/j.solener.2022.03.069>.
- [20] N. B. Khedher, "Experimental Evaluation of a Flat Plate Solar Collector Under Hail City Climate," *Engineering, Technology & Applied Science Research*, vol. 8, no. 2, pp. 2750–2754, Apr. 2018, <https://doi.org/10.48084/etasr.1957>.
- [21] T. Fang, D. Fang, and B. Yu, "Carbon emission efficiency of thermal power generation in China: Empirical evidence from the micro-perspective of power plants," *Energy Policy*, vol. 165, Jun. 2022, Art. no. 112955, <https://doi.org/10.1016/j.enpol.2022.112955>.
- [22] G. Wang, Y. Chao, T. Jiang, and Z. Chen, "Facilitating developments of solar thermal power and nuclear power generations for carbon neutral: A study based on evolutionary game theoretic method," *Science of The Total Environment*, vol. 814, Mar. 2022, Art. no. 151927, <https://doi.org/10.1016/j.scitotenv.2021.151927>.
- [23] K. Almutairi, M. Alhuyi Nazari, M. Salem, M. M. Rashidi, M. El Haj Assad, and S. Padmanaban, "A review on applications of solar energy for preheating in power plants," *Alexandria Engineering Journal*, vol. 61, no. 7, pp. 5283–5294, Jul. 2022, <https://doi.org/10.1016/j.aej.2021.10.045>.
- [24] M. Murugan *et al.*, "An overview on energy and exergy analysis of solar thermal collectors with passive performance enhancers," *Alexandria Engineering Journal*, vol. 61, no. 10, pp. 8123–8147, Oct. 2022, <https://doi.org/10.1016/j.aej.2022.01.052>.
- [25] H. Yan, X. Li, M. Liu, D. Chong, and J. Yan, "Performance analysis of a solar-aided coal-fired power plant in off-design working conditions and dynamic process," *Energy Conversion and Management*, vol. 220, Sep. 2020, Art. no. 113059, <https://doi.org/10.1016/j.enconman.2020.113059>.
- [26] C. Li, R. Zhai, and Y. Sun, "Thermal and economic performances comparison of different pulverized coal power systems augmented by solar trough or tower technologies," *Case Studies in Thermal Engineering*, vol. 34, Jun. 2022, Art. no. 102009, <https://doi.org/10.1016/j.csite.2022.102009>.
- [27] M. Ghazouani, M. Bouya, M. Benaissa, K. Anoune, and M. Ghazi, "Thermal energy management optimization of solar thermal energy system based on small parabolic trough collectors for bitumen maintaining on heat process," *Solar Energy*, vol. 211, pp. 1403–1421, Nov. 2020, <https://doi.org/10.1016/j.solener.2020.10.074>.
- [28] D. Guerraiche, K. Guerraiche, Z. Driss, A. Chibani, S. Merouani, and C. Bougriou, "Heat Transfer Enhancement in a Receiver Tube of Solar Collector Using Various Materials and Nanofluids," *Engineering, Technology & Applied Science Research*, vol. 12, no. 5, pp. 9282–9294, Oct. 2022, <https://doi.org/10.48084/etasr.5214>.
- [29] C. Huang, H. Hou, E. Hu, M. Liang, and Y. Yang, "Impact of power station capacities and sizes of solar field on the performance of solar aided power generation," *Energy*, vol. 139, pp. 667–679, Nov. 2017, <https://doi.org/10.1016/j.energy.2017.07.169>.
- [30] R. Zieba Falama *et al.*, "A comparative study based on a techno-environmental-economic analysis of some hybrid grid-connected systems operating under electricity blackouts: A case study in Cameroon," *Energy Conversion and Management*, vol. 251, Jan. 2022, Art. no. 114935, <https://doi.org/10.1016/j.enconman.2021.114935>.
- [31] Al Toukhi, "Arar Gas Turbine Power Plant," Saudi Electricity, GDPE14932PP-MP, Mar. 2022.
- [32] "Saudi Arabia Powerplants Output, CO2 and Intensity," *KAPSARC Data Portal*. <https://datasource.kapsarc.org/explore/dataset/saudi-arabia-powerplants-output-co2-and-intensity/analyze/>.